Exp Brain Res (2014) 232:2105–2119
DOI 10.1007/s00221-014-3901-5

RESEARCH ARTICLE

Neural representation of muscle dynamics in voluntary movement control

Christopher J. Hasson

Received: 21 August 2013 / Accepted: 2 March 2014 / Published online: 26 March 2014

Abstract Several theories of motor control posit that the nervous system has access to a neural representation of muscle dynamics. Yet, this has not been tested experimentally. Should such a representation exist, it was hypothesized that subjects who learned to control a virtual limb using virtual muscles would improve performance faster and show greater generalization than those who learned with a less dynamically complex virtual force generator. Healthy adults practiced using their biceps brachii activity to move a myoelectrically controlled virtual limb from rest to a standard target position with maximum speed and accuracy. Throughout practice, generalization was assessed with untrained target trials and sensitivity to actuator dynamics was probed by unexpected actuator model switches. In a muscle model subject group ($n = 10$), the biceps electromyographic signal activated a virtual muscle that pulled on the virtual limb with a force governed by muscle dynamics, defined by a nonlinear force–length–velocity relation and series elastic stiffness. A force generator group ($n = 10$) performed the same task, but the actuation force was a linear function of the biceps activation signal. Both groups made significant errors with unexpected actuator dynamics switches, supporting task sensitivity to actuator dynamics. The muscle model group improved performance as fast as the force generator group and showed greater generalization in early practice, despite using an actuator with more complex dynamics. These results are consistent with a pre-existing neural representation of muscle dynamics, which may have offset any learning challenges associated with the more dynamically complex virtual muscle model.

Keywords Virtual limb · Muscle mechanics · Motor learning · Voluntary movement control · Muscle dynamics · Nervous system · Neural representation

C. J. Hasson (✉)
Department of Physical Therapy, Movement and Rehabilitation Sciences, Neuromotor Systems Laboratory, Northeastern University, 360 Huntington Avenue, 301 Robinson Hall, Boston, MA 02115-5005, USA
e-mail: c.hasson@neu.edu

Introduction

The force produced by a muscle in response to neural input is dependent on the length and velocity of the muscle fibers, as well as the stiffness of the elastic tissue in series with the fibers (Hill 1938; Gordon et al. 1966; Bahler 1967). Muscle dynamics, characterized by force–length, force–velocity, and force–extension relations, play an important role in human movement (Hof 2003). Most prominently, they allow muscles to provide zero-delay compensation for mechanical perturbations, increasing the stability of the musculoskeletal system (Gerritsen et al. 1998; Kubow and Full 1999). Muscle dynamics also permit the storage and release of elastic energy, increasing the efficiency of movement (Cavagna 1977; Asmussen and Bonde-Petersen 2008).

While beneficial in these respects, muscle dynamics may pose a challenge for the nervous system in voluntary movement control: how to predict the force a muscle will produce in response to a neural input (Jordan and Rumelhart 1992; Miall et al. 1993), or conversely, determine the neural input needed to produce a desired force (Kawato 1990; Wolpert and Kawato 1998). The ability to perform this "neuromuscular transform" (Hooper and Weaver 2000) would be particularly advantageous when sensory information is delayed and/or unreliable (Wolpert and Ghahramani 2000). However, the transform is not trivial, as it

requires knowledge of muscle dynamics in addition to the current state of the musculoskeletal system (Kistemaker et al. 2013). Several theories of motor control posit that the nervous system has knowledge of muscle dynamics and can perform this transform, such as theories involving force control (Ostry and Feldman 2003) as well as optimal feedback control (Todorov and Jordan 2002b). Other theoretical paradigms, such as the equilibrium-point hypothesis (Feldman 1966), do not require this transformation and instead rely on the control of muscle length-activation thresholds and spinal reflexes. Nevertheless, whether the nervous system is capable of performing the neuromuscular transform remains an open question.

In contrast to muscle dynamics, neural representations of limb dynamics have been experimentally probed by several investigators (e.g., Atkeson 1989; Conditt et al. 1997). Healthy adults compensate for the effects of joint-interaction torques when reaching (Kurtzer et al. 2008) and adapt to altered limb dynamics (Sainburg et al. 1999). There is also evidence that the nervous system can readily adapt to new dynamic challenges presented by external objects, which range from simple rigid objects (Flanagan and Wing 1997), to mass-spring objects (Dingwell et al. 2002; Svinin et al. 2006), to objects with nonlinear dynamics such as modeled cups of coffee (Hasson et al. 2012). Considering these reports, it is plausible that the nervous system also accounts for muscle dynamics; however, there is little empirical evidence in support of this inference due to the difficulty of manipulating muscle dynamics in living humans (Fig. 1a). While it is a relatively simple matter to alter limb dynamics, for instance by adding an external mass to a limb, changing muscle dynamics properties, such as the intrinsic series elasticity of an individual muscle, is more difficult.

There are at least two approaches to overcoming the challenge of manipulating muscle dynamics in living humans. The first is to have humans interface with an artificial replacement limb that includes models of muscle dynamics that can be explicitly defined and manipulated to probe neural representations (Fig. 1b). For the artificial limb to function as a true "replacement," the neural connections to the original limb must be disconnected and new connections made to the artificial limb. This is conceptually similar to an amputee with a myoelectrically controlled prosthetic limb (Kuiken et al. 2004). However, for the purposes of the present study, this approach is not ideal due the variability introduced by cortical reorganization prior to receipt of the prosthetic (Hall et al. 1990). The second approach is to connect a virtual myoelectrically controlled limb to the human in an additive manner (Fig. 1c), keeping the original limbs intact (e.g., Manal et al. 2002; Erdemir et al. 2007; Cheng and Loeb 2008; de Rugy et al. 2012). The latter approach is taken in the present study.

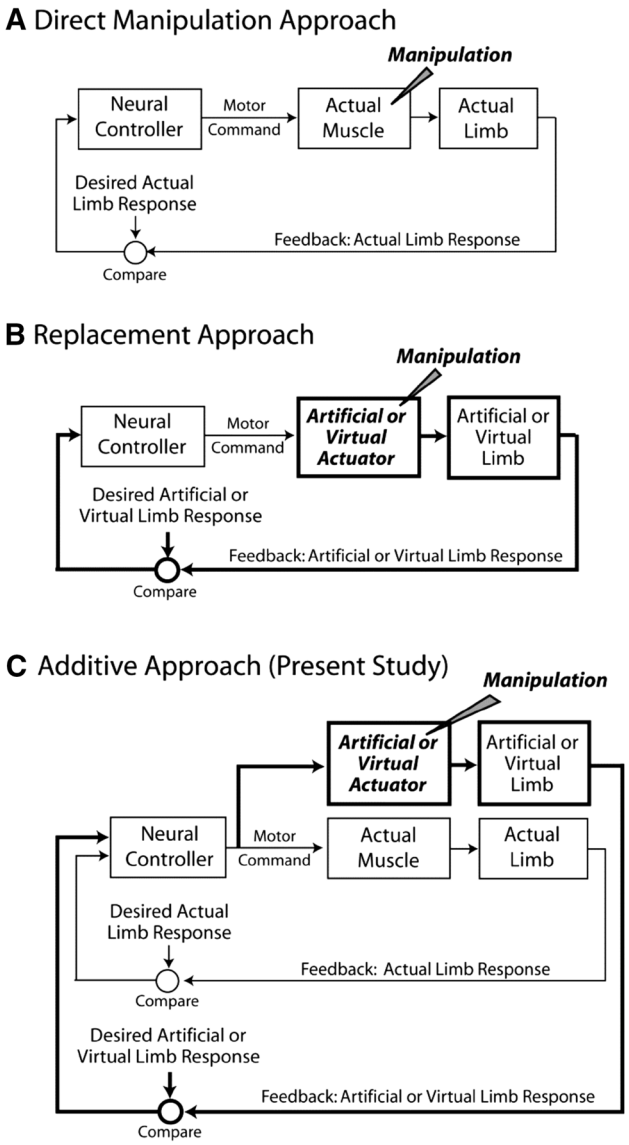

Fig. 1 Different approaches to testing the hypothesis that the nervous system has knowledge of muscle dynamics. **a** A highly simplified diagram of the human neuromotor system showing the most direct experimental approach: invasively manipulate muscle dynamics properties. **b** A "replacement approach," in which an artificial or virtual limb replaces the actual limb and the properties of the artificial/virtual limb's "muscles" are manipulated. **c** An additive approach, which was taken in the present study. Here, subjects are given a virtual limb to control but their actual limb remains intact. Consequently, an additional sensory feedback channel is created

To test for neural representations of muscle dynamics, two groups of subjects were tasked with learning to control the same myoelectrically controlled virtual limb, but unknown to the subjects, each group used a different actuator model. In a *muscle model* group, the measured muscle activity served as an activation signal to a virtual muscle model, which produced a force that was a nonlinear function of a contractile element's (CE) length and velocity and

the stiffness of a series elastic element (SEE). A second *force generator* group performed the same task, but their muscle activity was linearly mapped from an activation signal to a force that actuated the virtual limb, a mathematically simpler transformation.

It was hypothesized that preexisting knowledge of muscle dynamics would allow subjects who learned to control a virtual limb using virtual muscles to improve performance faster and show greater generalization than those who learned with a non-muscle-like virtual force generator. On the other hand, if subjects approach the task as *tabula rasas*, i.e., with no existing neural representations or knowledge of muscle dynamics, then compared to the muscle model group, the force generator group should learn the task faster and show better generalization due to simpler dynamics. These expectations are supported by recent evidence that simpler models of dynamics require less time to learn than more complex ones (Narain et al. 2013).

Methods

Overview

Subjects practiced a goal-directed task with a virtual limb driven by their muscle activity. The virtual limb was an intentionally simplified representation of a human limb: a single degree-of-freedom limb segment with a single actuator. In a muscle model group (age: 25 ± 5 years; height: 1.68 ± 0.17 m; weight: 83 ± 18 kg), online measurements of muscle activity served as an input to a muscle model actuator that drove the virtual limb. In a force generator group (age: 23 ± 3 years; height: 1.67 ± 0.22 m; weight: 78 ± 25 kg), the virtual limb was driven by an actuator that produced a force proportional to the muscle activity. There were 10 subjects in each group with group assignment randomized. Subjects were told that their muscle activity would move the virtual limb, but were not given specifics about the actuator dynamics. All subjects were healthy and free from cognitive, musculoskeletal, and neurological impairments. Prior to participation, subjects read and signed an informed consent form approved by the local institutional review board.

Experimental setup

Apparatus

Subjects sat on a chair and faced a computer monitor with their right arm at their side, their upper arm aligned vertically with their torso, and their elbow at 90° of flexion (0° = fully extended). All subjects were right-hand dominant. Subjects grasped a bar with their hand supinated in a biceps curl position. The bar was fixed and anchored to the floor so that subjects could pull against the immobile bar. A stiff foam pad was placed under the forearm, supporting its weight. Subjects' arms remained in this fixed position throughout the experiment. This fixed position was chosen to minimize electromyographic artifacts due to sliding of muscles under surface-mounted electrodes, which would be exaggerated with actual limb movement (Potvin 1997).

Muscle activity measurement

Biceps muscle activity was monitored with a wireless electromyography system (Myon AG, Baar, Switzerland; bandwidth: 5–1,000 Hz, latency: 16 ms). Prior to placement of Ag/AgCl circular disposable electrodes (Kendall™/Arbo™ H124SG, Covidien, UK, Commercial Ltd.,), the skin was shaved, rubbed with an abrasive gel (NuPrep®, Weaver and Company, Aurora, CO, USA), and cleaned with alcohol. Electrodes were positioned in a bipolar configuration in the center of the biceps muscle belly oriented parallel to the fibers with an inter-electrode distance of 2.0 cm. After placement, the electrodes were covered with elastic wrap (Coban™, 3M™, St. Paul, MN, USA). Amplified muscle activity was rectified and filtered using an analog fifth-order low-pass Butterworth filter (MAX280; Maxim Integrated Products, Inc., San Jose, CA, USA) with a cutoff frequency of 4 Hz.

Musculoskeletal model

Virtual limb

A virtual limb was created in MATLAB® (MathWorks®, Natick, MA, USA). The limb was a single rigid segment that could rotate about a hinge joint (Fig. 2a). Although controlled with biceps activity, the virtual limb was not intended to be "arm," i.e., a variety of virtual limb geometrical and inertial properties could be used to test the hypothesis. The segment length was 0.435 m, and the moment of inertia about the axis of rotation was 0.5 kg m^2 (Hatze 1975). A lower leg inertial value was used because higher inertia (relative to the forearm) made the virtual limb easier to control. The virtual limb was moved by a torque from an actuator that originated from a fixed position 0.423 m to the right of the limb axis of rotation, and inserted on the limb 0.04 m along its length from the axis of rotation (Fig. 2a). These insertion points were chosen so the actuator would experience a physiologically plausible range of length changes, i.e., about 30 mm over 60° of limb movement (Fellows and Rack 1987); they do not correspond to specific anatomical landmarks. These virtual limb properties remained the same for all subjects.

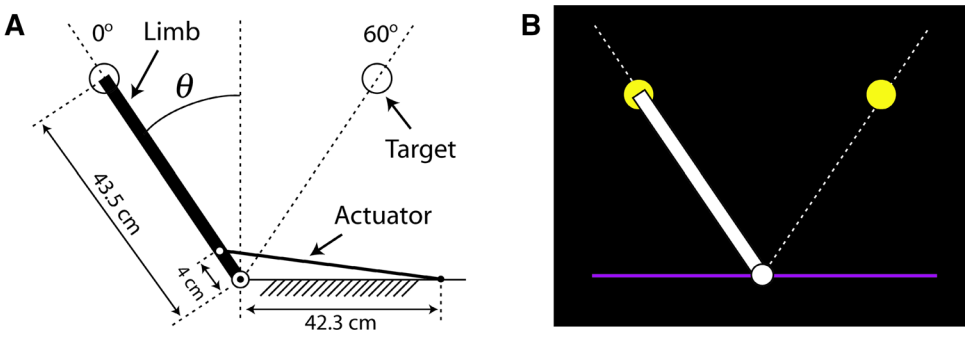

Fig. 2 **a** Schematic of virtual limb with actuator. **b** Screenshot of visual display with the virtual limb in the starting position

Friction model

A frictional torque T_F was added to mimic a limb rotating on a planar surface, based on the rotational friction model used in MATLAB® Simscape™. This allowed the virtual limb to slow down, because a single pulling actuator can only accelerate the virtual limb in one direction. The friction model also prevented the virtual limb from moving from rest due to spurious electromyographic signals. The friction model was a modified version of that used by Armstrong and de Wit (1996). This model assumes that T_F is linearly proportional to the velocity up until an angular velocity threshold ω_{TH} (0.005 rad/s), which makes the virtual limb "stick" at very low velocities. Below ω_{TH}

$$T_F = \omega \frac{f\omega_{TH} + \left[T_C + (T_{BRK} - T_C)\exp\left(-c_v\omega_{TH}\right)\right]}{\omega_{TH}} \quad (1)$$

and above ω_{TH}

$$T_F = \left[T_C + (T_{BRK} - T_C)\exp\left(-c_v|\omega|\right)\right]\mathrm{sign}(\omega) + f\omega. \quad (2)$$

where ω is the virtual limb angular velocity, T_{BRK} is the breakaway friction torque (0.5824 Nm, representing a coefficient of static friction μ_s of 0.025). T_C is the Coulomb friction torque (set to 80 % of T_{BRK}; $T_C = 0.4659$ Nm), f is a viscous friction coefficient that was set to 1.5 Nm/rad/s, in the range of limb damping estimates of Hatze (1975), and c_v is a coefficient that describes the transition approximation between static and Coulomb frictions ($c_v = 10$ rad/s). Note that for the purposes of the present study, the exact values of the friction model coefficients are inconsequential. An extremely large coefficient of static friction would not be desirable, but a range of values could have been used.

Virtual limb passive dynamics

An elastic torque T_P acting in parallel constrained the range of motion of the limb, mainly to prevent the virtual limb from circling around the axis of rotation, such that

$$T_P = ab^{(\theta+c)} - ab^{(-\theta+c)} \quad (3)$$

where $a = 1.0 \times 10^{-15}$, $b = 0.65$, and $c = -10.6$. Pilot work showed that the virtual limb rarely contacted this boundary; at most only a few times throughout a practice session. The selected values were found through trial and error so that the T_P would not interfere with the movement until the limb moved close to the right horizontal (120°), after which T_P rose quickly to prevent the limb from moving further.

Virtual limb simulation

The hardware rectified and low-pass filtered biceps muscle activity was sampled using an analog-to-digital converter (PCI-6289; National Instruments, Austin, TX, USA). Data were sampled at 75 Hz and synced to the monitor refresh rate. The simulation steps, illustrated in Fig. 3, were as follows: Step 1: the rectified and low-pass filtered muscle activity (FEMG) was converted to a normalized excitation signal ranging from zero to one. The resting muscle activity level ($FEMG_{REST}$) was the average FEMG at rest (see "Calibration" section below for details on calibration protocol). Because of measurement noise, $FEMG_{REST}$ could not be used to define when the muscle was "off" without introducing spurious "on" signals. This was avoided using a threshold of 35 % above $FEMG_{REST}$ to specify when a muscle is "on" or "off," called $FEMG_{THRESH}$

$$FEMG_{THRESH} = FEMG_{REST} + 0.35\ FEMG_{REST}. \quad (4)$$

Because any activity below $FEMG_{THRESH}$ was considered "noise," it was set equal to $FEMG_{THRESH}$, i.e.,

$$\text{if } FEMG < FEMG_{THRESH}, \quad \text{then}$$
$$FEMG = FEMG_{THRESH}. \quad (5)$$

The 35 % excitation threshold was chosen by trial and error. A threshold that is too low would lead to spurious activations of the virtual limb actuator, but a threshold that is too high would reduce the ability of subjects to exert fine control over the actuators. To scale subject's muscle activity, the threshold $FEMG_{THRESH}$ was subtracted from FEMG and this quantity was divided by the maximum FEMG

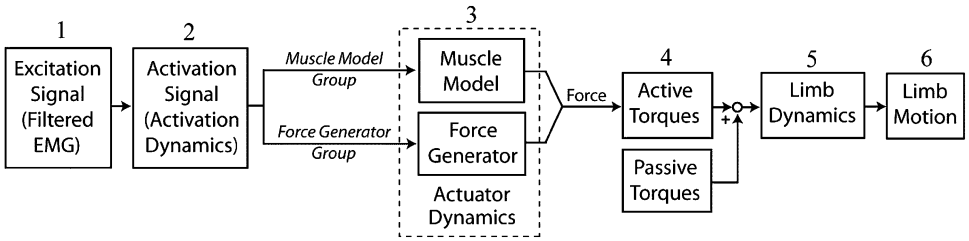

Fig. 3 Flowchart depicting simulation procedure for the virtual limb. All elements of the simulation were identical for two groups of subjects, except for the model of the actuator that acted on the virtual limb. In one group, subjects' muscle activity served as an input to a muscle model, but in the other group, the muscle activity was mapped to a force generator (see text for details of each simulation step)

recorded during maximal voluntary contractions FEMG_{MVC} (see "Calibration" section for details). For proper scaling, $\text{FEMG}_{\text{THRESH}}$ was also subtracted from FEMG_{MVC}. This process gave a scaled excitation signal $\text{FEMG}_{\text{SCALED}}$ that ranged from 0 to 1, given by

$$\text{FEMG}_{\text{SCALED}} = (\text{FEMG} - \text{FEMG}_{\text{THRESH}})/(\text{FEMG}_{\text{MVC}} - \text{FEMG}_{\text{THRESH}}). \quad (6)$$

Step 2: the normalized excitation signal $\text{FEMG}_{\text{SCALED}}$ was converted to activation by excitation-activation dynamics, represented as a first-order process with activation and deactivation time constants of 10 and 50 ms, respectively (Winters and Stark 1988). The equations governing this process are detailed in Hasson and Caldwell (2012). Step 3: depending on subject group assignment, the activation signal was converted to a force via either a force generator, which generated a force proportional to the activation signal, or via a nonlinear muscle model, which produced force according to the muscle dynamics, defined by force–length, force–velocity, and force–extension relations (see "Muscle model details" section). Step 4: the force generator/muscle model force was multiplied by a moment arm to produce an active torque T_A. The moment arm MA is given by $\text{MA} = dL/d\theta$ (An et al. 1983), where L is the length of the actuator, computed as the distance between the origin and insertion of the virtual muscle. Step 5: the virtual limb's angular acceleration was computed by dividing the net joint torque ($T_A + T_P + T_F$) by the limb moment of inertia, and Step 6: numerical integration was performed via a fourth-order Runge–Kutta algorithm (Press et al. 2007) to compute the angular velocity and displacement of the virtual limb.

Visual display

A visual display was created with vector-based graphics with OpenGL functions from the Psychotoolbox library of MATLAB® functions (Brainard 1997). The virtual limb was drawn as a simple rotating line segment (Fig. 2b). A horizontal magenta reference line was drawn through the limb rotation axis. The starting and target positions were marked by yellow circles drawn along the arc of the limb movement path.

Muscle model details

For muscle model actuation, the motive force acting on the virtual limb was produced by a classic two-component Hill-type muscle model (Hill 1938; Zajac 1989), which received an excitatory input based on the measured muscle activity (see Fig. 3). This model (Fig. 4) included a CE and a SEE. The behavior of the CE was defined by a nonlinear force–length and force–velocity relation. The SEE behaved as a nonlinear spring according to a force–extension relation. Equations governing the behavior of the model are detailed in Hasson and Caldwell (2012).

For the purpose of testing the hypothesis, the key requirement was for a muscle model that reproduced the basic behavior of muscle: the *exact* parameters of the muscle model were not of critical importance. For example, the muscle could have been modeled as one that contracts fast or slow, is more or less compliant, or is weak or strong. The properties of the muscle model were purposely made to be dissimilar from those of the muscle subjects used to control the virtual limb, the biceps brachii. This more rigorously tests whether there is an internal representation of muscle dynamics that generalizes across muscles. The gastrocnemius was chosen as the muscle model to be consistent with the chosen inertial properties (which are of a lower leg) and also due to the availability of muscle mechanical property estimates. The CE and SEE properties (i.e., force–length, force–velocity, and force–extension relations) were based on the values reported in Hasson and Caldwell (2012). These properties are illustrated in Fig. 4 and include: the optimal CE length L_0 (5.8 cm), the width of the force–length relation W (0.8), the SEE slack length L_S (0.285 cm), three coefficients specifying the CE force–velocity relation a/P_0, b/L_0, and ε (0.29, 3.51 s^{-1}, and 2.48, respectively), and two coefficients describing the SEE force–extension relation, α and β (409 and 12, respectively). The maximal isometric force F_0 of the muscle was set to 1,400 N, in the

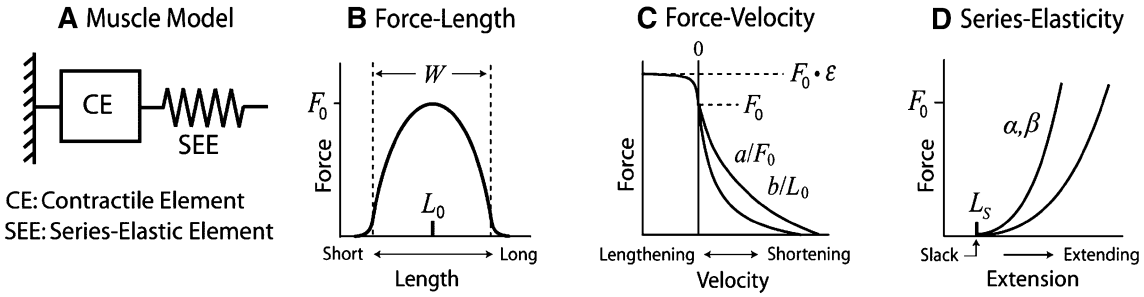

Fig. 4 Two-component muscle model (**a**) with force–length (**b**), force–velocity (**c**), and force–extension relationships (**d**), which together mediate the translation of a neural activation signal into force. Several parameters define the relationships: the maximal isometric force F_0, the optimal CE length L_0 and width of the force–length relation W, coefficients specifying the CE force–velocity relation, a/P_0, b/L_0, and the eccentric plateau ε, coefficients describing the shape of the SEE force–extension relation α and β, and the SEE slack length L_S

range of young male gastrocnemius estimates in Hasson and Caldwell (2012). Pilot work showed that in the virtual limb task, this F_0 required peak muscle excitation amplitudes of about 20 % of maximum, which was similar to that used by Gordon and Ferris (2004) to prevent fatigue.

Force generator details

For force generator actuation, the virtual limb was moved by a force that was a linear function of an activation input derived from the measured muscle activity. The maximal force capability (F_0) of the actuator was the same as the muscle model (1,400 N). Aside from the different actuator dynamics, all other aspects of the experimental task and virtual limb were the same as for the muscle model group.

Experimental procedures

Calibration

After electrode placement, a calibration procedure was performed to scale muscle activity measurements for each subject. Two resting trials were captured in which subjects relaxed their biceps for 2 s. The average hardware-filtered resting muscle activity across these two trials was defined as $\text{FEMG}_{\text{REST}}$. Next, three maximum voluntary contractions were performed with 30-s rest periods. Subjects were told to pull against the support bar as hard as possible and maintain the effort for 3 s. The highest value of the rectified and filtered data across the three trials gave FEMG_{MVC}. These calibration factors were then used to calculate $\text{FEMG}_{\text{SCALED}}$, which activated the muscle model/force generator (Eq. 6).

Virtual limb task

Subjects were instructed to use their biceps muscle activity to move the virtual limb clockwise from the starting position (0°) and bring it to a stop in a target circle (Fig. 2b) as quickly as they could (subjects' actual limbs did not move). Subjects were told to stop the virtual limb as close to the target circle center as possible and that the trial ends when limb motion ceases (<4°/s for 0.3 s). For reinforcement, the target circle turned from yellow to green when the angular error was within a success threshold of ±4° from the target center. If the limb was brought to stop within the target (±4°), a "ding" sounded signaling success; otherwise a "buzz" sounded indicating that the limb was not on-target. After each trial, the movement time was displayed, defined as the time from when the limb left the starting circle to when the limb stopped. Subjects' fastest successful movement time was also displayed, and if a given trial exceeded this time the program "applauded" and the fastest time was updated.

Protocol

To test the hypothesis, the experimental protocol assessed subject's learning rate and ability to generalize their skill. Subjects were asked to practice the virtual limb task for four blocks of 69 trials each (Blocks 1–4; 276 total trials). *In standard target* trials, the target circle was located 60° clockwise from the starting circle (Fig. 2a). To evaluate generalization, in each block, the target was moved in an alternating fashion every 10 trials to a *near-target* position (45°) or a *far-target* position (75°). A blocked experimental design, where subjects practice with all standard targets and then switch to all near or far targets, was not used as this would have eliminated the ability to examine changes in generalization as learning progressed—a key focus of the present study.

The protocol also tested the sensitivity of task performance to the actuator dynamics. This is a check to confirm that the differences in the actuator models are not trivial, i.e., a failure to plan for the right actuator model

should cause a large error. For this purpose, in each block, *dynamics-switch* trials were inserted on trials 25, 45, and 65. In these trials, the actuator model was switched: the muscle model group was switched to a force generator and vice versa (the target remained at 60°). Subjects were not informed of the switches, and the virtual limb visual feedback remained unchanged. For the entire practice session, there were 240 standard target trials, 12 near-target shifts, 12 far-target shifts, and 12 dynamics-switch trials.

Data analysis

Dependent measures

The three dependent measures were as follows: (1) movement time, (2) absolute angular error, and (3) performance. Movement time is the time from when the limb left the starting circle to when it came to rest (<4°/s for 0.3 s). The absolute angular error is the absolute value of the angular difference between the virtual limb's final position and the target center. The performance measure is a composite of movement time and error since subjects could trade-off either quantity, i.e., they could move slower and be more accurate, or vice versa. The performance measure is similar in concept to the "skill" measure used by Reis et al. (2009), i.e., performance is low for slow and inaccurate movements, and high for fast and accurate movements. However, Reis et al. empirically defined the speed-accuracy trade-off for each subject, which was not done in the present study. The performance measure calculation involved several steps: (1) To correct for differing units of measure, movement time and error was scaled to a range covering 95 % of the data across practice (error range: 0°–13°; movement time range: 0.8–2.3 s). (2) The scaled measures were represented as two orthogonal axes on a "performance" plot (Fig. 5). The scaled movement time and error gives a single point for each trial; the distance of this point from the origin represented performance. (3) The performance measure was multiplied by −1 so an increase represented improved performance, and (4) the measure was normalized to the performance level at the very beginning of practice by shifting the measure by an amount equal to the average performance value for the first 5 trials (averaged across both groups).

Data reduction

After movement time, absolute error, and performance variables were computed, the standard target trials (60°; $n = 240$) were separated from the interleaved near (45°; $n = 12$), far (75°; $n = 12$), and dynamics-switch (60°; $n = 12$) trials. For the standard trials, data were averaged in non-overlapping 20 trial bins (12 bins) for each subject. To avoid averaging out differences in the very early trials, in which rapid changes occurred, the first five trials were averaged separately, giving 13 total bins. Exponentials were fit to each subject's binned performance data (13 points) using a nonlinear least squares method; the time constant reflected the rate of performance improvement.

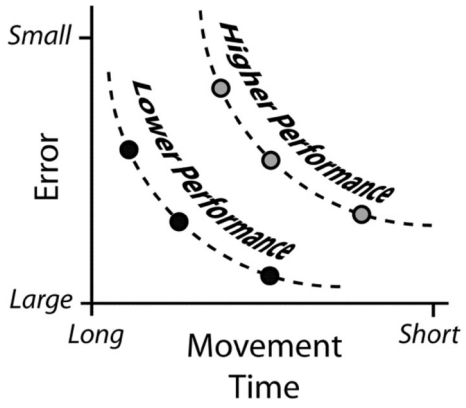

Fig. 5 Schematic of the performance measure, which combines movement time (speed) and error (accuracy). Low performance is characterized by long movement times and/or large errors (*black circles*); high performance by short movement times and/or small errors (*gray circles*)

The near-/far-target and dynamics-switch trials were compared with the standard trials to assess generalization and sensitivity to actuator dynamics, respectively. Changes in skill with practice were assessed by comparing the early near, far, and dynamics-switch trials with the early standard trials, and vice versa for the late trials, i.e., the comparison was on a block-by-block basis. In the first block of 69 practice trials, the three near-target trials were averaged and subtracted from the average for the *same* block of standard practice trials. This process was repeated for the far-target and dynamics-switch trials, and for the second, third, and fourth practice blocks. Comparing the near, far, and dynamics-switch trials on a block-by-block basis reduces the bias due to cumulative learning effects.

Dynamics-switch trial analysis

The muscle model to force generator switch should cause subjects to overshoot the target since force rises faster with muscle dynamics removed, and there is no way to actively brake or pull back the virtual limb. Such errors, if significant, would indicate sensitivity to actuator dynamics. In the reverse situation, i.e., the force generator to muscle model switch, the force produced by the actuator should rise slower than expected due to unanticipated muscle dynamics and cause an undershoot. However, an undershoot can be corrected to reduce end-point errors, masking actuator sensitivity. This asymmetrical behavior of the dynamics-switch

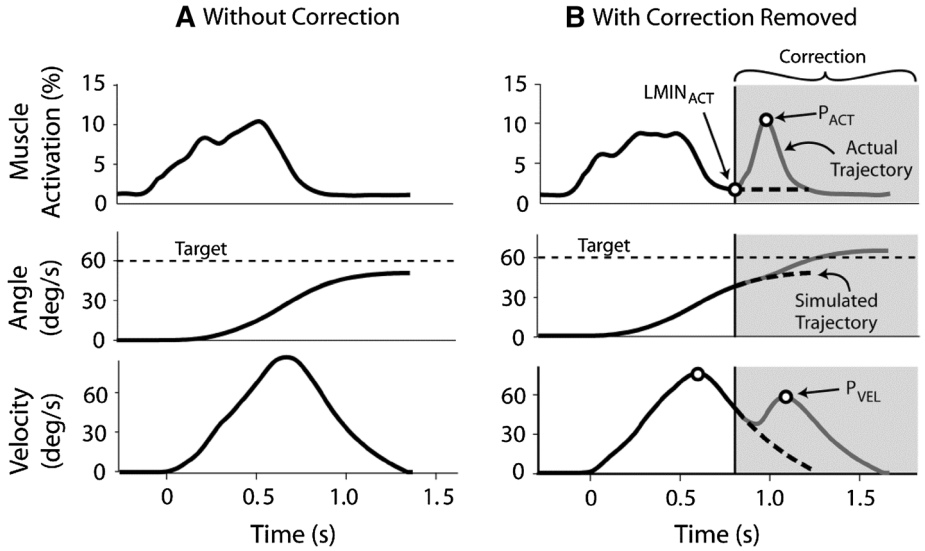

Fig. 6 Example of force generator to muscle model dynamics-switch trials in which the subject made a single uncorrected movement (**a**) and one with a correction (**b**). A correction was characterized by a double-peaked virtual limb angular velocity profile. Working backward in time from the second velocity peak (P_{VEL}), the peak activation (P_{ACT}) was identified, followed by the minimum activation prior to the second activation peak ($LMIN_{ACT}$). Thresholds were used to prevent misidentification. The movement of the virtual limb was simulated from $LMIN_{ACT}$ onward to see where the limb would have stopped without the corrective action (*dashed lines*)

trials is because subjects could see the virtual limb and attempt to correct movement errors. Typically, studies that use "catch" trials, in which a manipulation is turned off or abruptly changed, remove visual feedback of the end-effector position (Smith et al. 2006; Shmuelof et al. 2012). Visual feedback was not removed during the dynamics-switch trials because it would otherwise be difficult to conclude whether an observed error was due to the altered actuator dynamics or the sudden absence of sensory feedback. In contrast to most human motor learning studies, *only* visual feedback of the virtual limb was available to subjects, and therefore, removal of this feedback served as a relatively large perturbation.

To address the correctible nature of the force generator to muscle model switch, a multistep procedure was used to detect the presence of corrective actions and simulate how the virtual limb would have moved if corrections were not made. This procedure is illustrated in Fig. 6. First, the MATLAB® function *findpeaks* was used to identify peaks in the virtual limb angular velocity profile. A corrective action was defined by the presence of more than one peak separated by at least 150 ms and 10°/s. If there was a correction, starting from the time of the second peak (P_{VEL}) and moving backward in time, the closest peak in the activation signal was selected (P_{ACT}). Moving further back in time, the next local minimum in the activation signal ($LMIN_{ACT}$) at least 5 % lower than the activation peak was selected. The position and velocity of the virtual limb at $LMIN_{ACT}$ was used as an initial condition and a simulation performed to see where the virtual limb would have come to rest if the corrective action was not taken (activation was assumed to remain at $LMIN_{ACT}$). Trials with the corrections removed were then incorporated into the statistical analysis.

Statistical analysis

A linear mixed-effects model with repeated measures was used to test for differences ($p < .05$) between the muscle dynamics and force generator groups. The dependent variables were movement time, absolute angular error, and performance. Fixed factors were group (muscle model or force generator) and practice; the subject identification number was a random factor. A Toeplitz covariance structure was used as this gave the lowest Akaike and Bayesian information criterions (Akaike 1974; Schwarz 1978). For each dependent variable, group differences within each block were tested with independent samples *t* tests. Group differences in the performance improvement rate, defined by the time constant of the exponential fit to the performance measure, were tested using an independent samples *t* test.

Results

The results are presented in three sections. The first presents data from individual subjects and describes the raw data. The second presents the group learning rate and generalization findings, which test the hypothesis. The third shows the

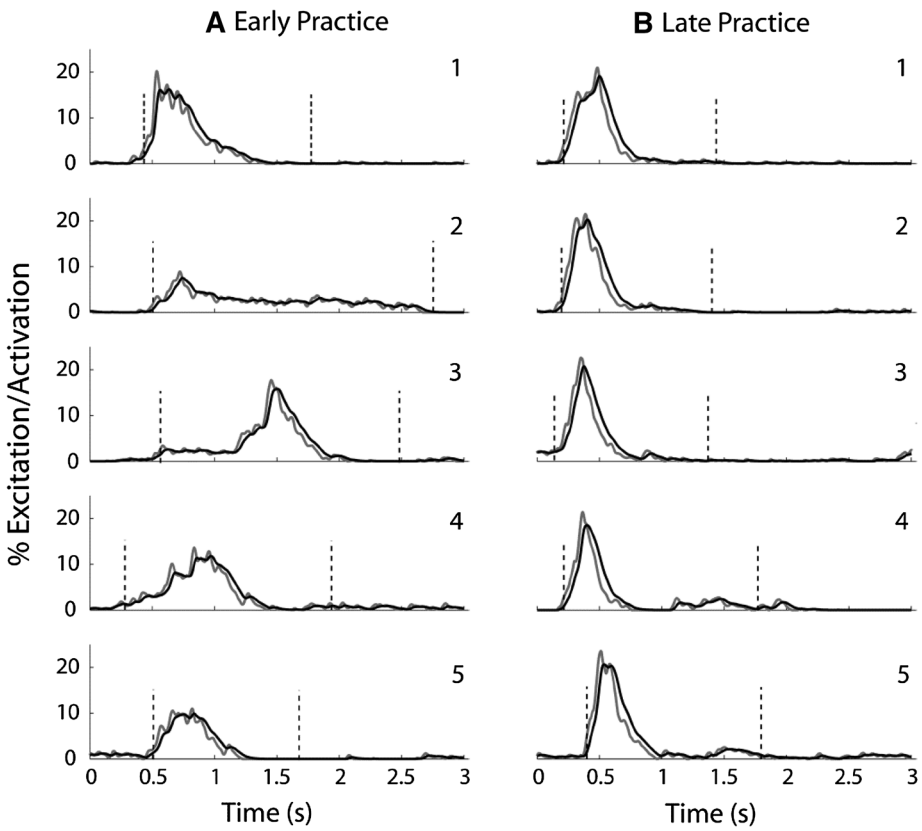

Fig. 7 Example of hardware-filtered biceps excitation (*gray line*) and computed-activation (*black line*) profiles for five trials in early (**a**) and late (**b**) practice for one subject in the muscle model group. The activation signals were used as control inputs to a muscle model that actuated a virtual limb. For reference, the *two dashed vertical lines* denote the onset and offset of virtual limb motion. Note that the end of virtual limb movement typically occurred sometime after the end of activation; during this period frictional forces brought the limb to a stop

results from the dynamics-switch trials, which quantified the sensitivity of the task to the actuator dynamics.

Muscular activity patterns and virtual limb kinetics and kinematics

Figure 7 shows hardware-filtered excitation signals (gray lines) recorded from the biceps muscle and corresponding activation profiles (black lines) for five trials in early and late practice for one subject in the muscle model group. As shown, the conversion from excitation to activation has a smoothing effect. The conversion to activation was done in both muscle model and force generator groups (Fig. 3; Box 2). Early practice trials (Fig. 7a) are marked by high-variability between-trials in both the amplitude and duration of muscle activity. These features became more consistent with practice (Fig. 5b). Virtual limb movement typically stopped with some delay after activation ceased (limb movement onset/offset indicated by vertical dashed lines). During this time, the modeled frictional forces acted on the virtual limb to bring it to a stop.

The virtual limb kinematics and muscle model CE kinematics and kinetics are shown for one muscle model group subject in Fig. 8. Twelve consecutive late standard target practice trials (of 240 total trials) are shown (A). For the near-target (B), far-target (C), and dynamics-switch (D) conditions, there were only 12 trials (all are shown). The subject shown in Fig. 8 was able to maintain accuracy on most trials for the near- and far-target trials (Fig. 8a, b). However, a large decrement in accuracy and increase in movement speed (steeper slope of angle vs. time) can be seen for many of the dynamics-switch trials (Fig. 8d). Of these, only two trials made it into the target region; however, these trials were associated with slower virtual limb movements.

The data presented in Fig. 8 also show how the CE experienced substantial changes in length and velocity, and therefore, the muscle model group had to contend with the nonlinear aspects of the muscle dynamics. Before the virtual muscle was activated, the CE was 27 % longer (1.27 L_0) than its optimal length. After activation, the CE shortened past the optimal length, and continued shortening throughout the movement, ending at lengths of 0.75, 0.57, and 0.43 L_0 for the near-, standard-, and far-target positions, respectively (assuming the limb is at rest on-target). The average maximum CE velocity was 1.25 ± 0.43, 2.17 ± 0.21, and 1.82 ± 0.52 L_0/s for the near-, standard-, and far-target positions, respectively (mean ± SD).

Task performance and generalization

For the standard target position, subjects decreased their movement time and absolute angular error with practice,

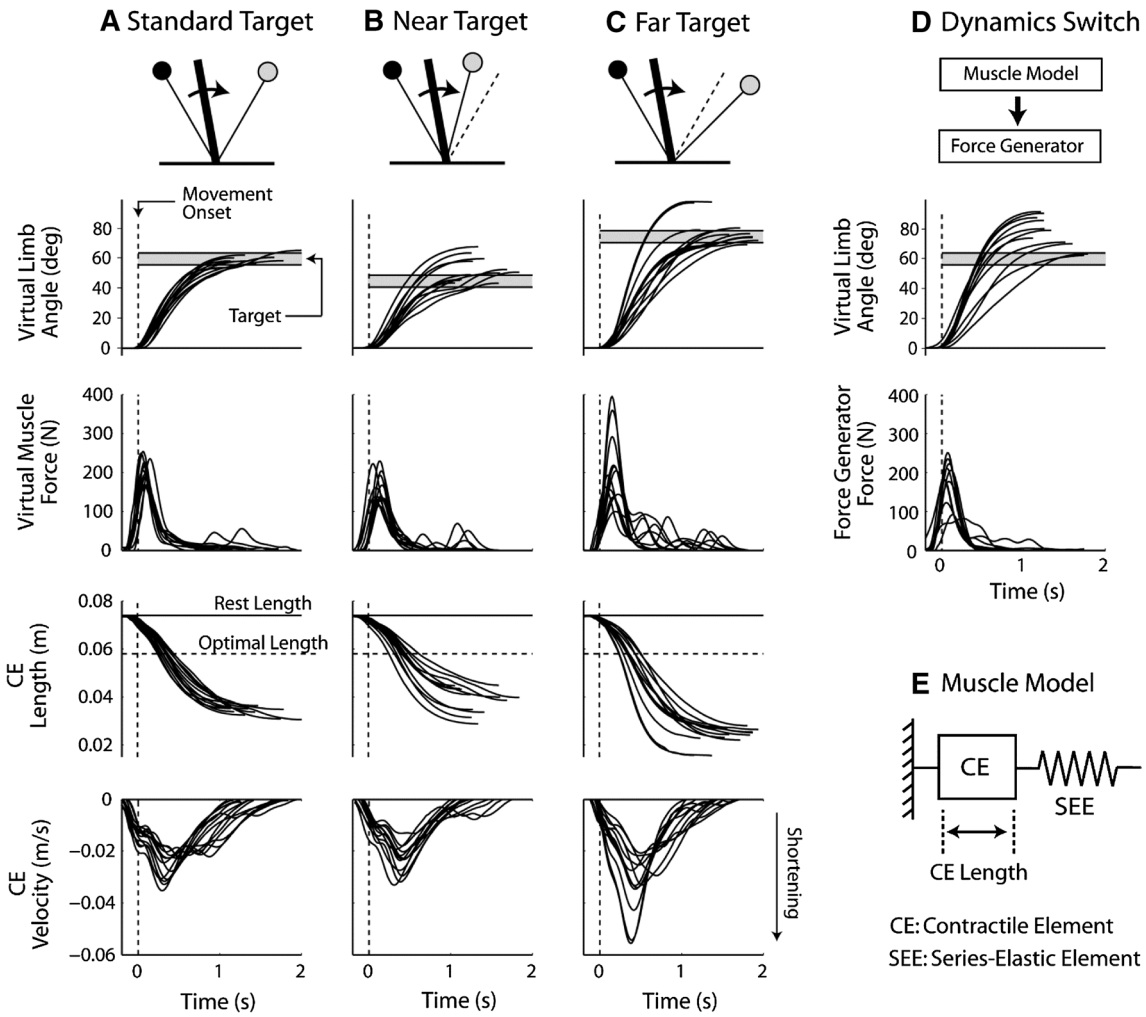

Fig. 8 Exemplar virtual limb angle and muscle model kinetics and kinematics for one subject in the muscle dynamics group in each of the four conditions. From *left* to *right*, *each column* represents trials with the standard target position (**a**; 12 consecutive late practice trials), interleaved trials with near and far targets (**b**, **c**), and trials in which the muscle model was unexpectedly replaced with a force generator (**d**). The length and velocity of the contractile element (CE) are shown, based on the muscle model shown in **e**. Data are aligned to the onset of the virtual limb movement

and hence, their performance increased (main effect of practice; $p < .001$ for all three measures; Fig. 9a). In these standard target trials, there were no differences between the muscle model (black bars) and force generator (gray bars) groups for movement time, error, and performance, and in neither group, did these measures change faster than the other ($p > .05$). The learning rate time constants for the fitted exponentials for both groups did not differ from each other (24.7 ± 11.2 vs. 19.0 ± 13.4 trials for muscle model and force generator groups, respectively; $p > .05$). The absolute angular speed of the virtual limb did not differ between the muscle dynamics and force generator groups (36 ± 5 vs. 35 ± 6°/s, respectively; $p = .768$) over the last 30 standard target trials. Similarly, the average maximum angular speed did not differ between the muscle dynamics and force generator groups (52 ± 6 vs. 52 ± 7°/s, respectively; $p = .889$) over the last 30 standard target trials.

To test generalization, the target shifted every 10 trials, alternating between near and far positions. Performance on these trials, relative to the standard target trials on the *same* practice block, is shown in Fig. 9b, c (i.e., the Block 1 near-target measures are relative to the Block 1 standard target measures, Block 2 near target is relative to Block 2 standard, and so on). For these relative measures, positive movement times and errors reflect slower and/or less accurate virtual limb actions compared to the standard target trials. A positive relative performance value reflects improved performance relative to the standard trials.

There were several differences in generalization between the muscle model and force generator groups in early practice (Block 1). Specifically, the muscle model group had

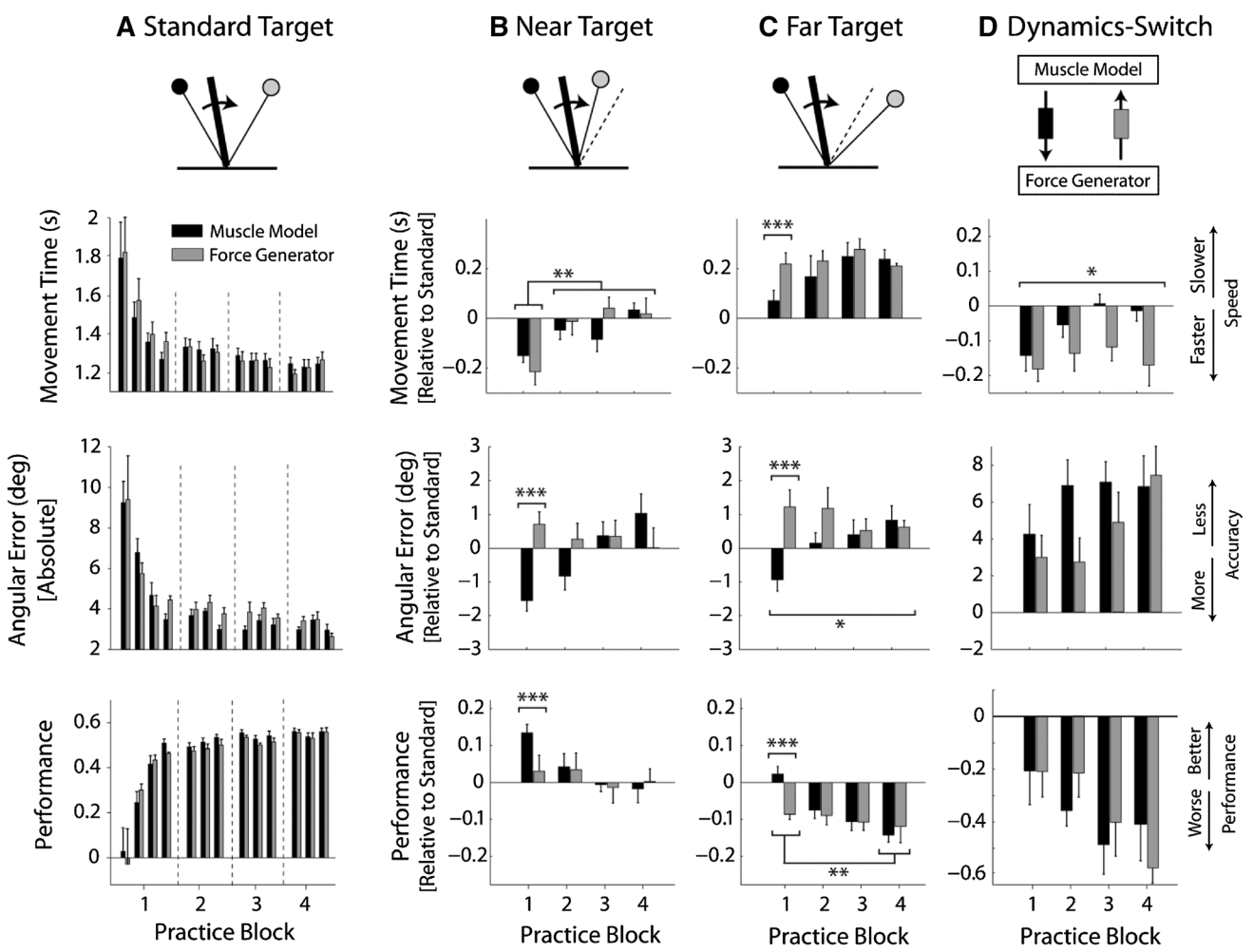

Fig. 9 Average movement time, absolute angular error, and performance for the muscle model (*black bars*) and force-generator (*gray bars*) groups. The performance measure combines both movement time and accuracy; a higher performance value reflects a movement that was faster and/or more accurate. For performance, values are normalized to the average performance in the first five trials across both groups. Results shown for trials with the standard target position (**a**) and interleaved generalization trials with the target in a near position (**b**) or a far position (**c**). Also shown are trials in which the actuator model in the muscle model group was unexpectedly switched to a force generator, and vice versa for the force generator group (**d**). The former switch generally caused target overshoots, and the latter undershoots. Because in the task an undershoot was correctible, the effects of the dynamics switch were masked. This was addressed by identifying and removing the corrections and simulating how the uncorrected movement would have unfolded. For **b**–**d**, the data are expressed relative to performance on the standard target trials averaged over the same period. For **b**–**d**: *significant main effect of group; **significant overall practice effects; ***significant group difference in a specific practice block. For the standard trials (**a**), all three measures had main effects of practice, but no group differences. Standard errors shown

smaller relative errors and greater relative performance for both near (error: $p = .005$; performance: $p = .048$) and far targets (error: $p = .003$; performance: $p = .041$). There were also significant overall practice effects. For the near-target practice, Block 1 had shorter relative movement times than Blocks 2–4 ($p = .004$), and for the far target, Block 1 had greater relative performance transfer than Block 4 ($p = .004$). An overall interaction was observed in the near-target condition, such that the relative error for the force generator group remained relatively constant, but the muscle model group relative error grew over practice ($p = .028$).

Dynamics-switch trials

Dynamics-switch trials were used to test the degree to which the task performance was sensitive to the properties of the actuators. In these trials, the actuator model was unexpectedly switched: muscle model to force generator and vice versa. The former switch caused target overshoots and the latter undershoots. While an overshoot could not be corrected, it was possible to correct an undershoot. Such corrective actions may mask the effects of the dynamics switch. This was addressed by identifying and removing corrective submovements for the force generator to muscle

model switch, and simulating the uncorrected movements. The results, with removed corrections, are shown in Fig. 9d. Subjects made significant errors on the dynamics-switch trials. For both groups, the movement time, error, and performance were all different from zero (significant model intercepts: $p < .001$). There were no group differences for error and performance ($p = .108$ and $p = .852$, respectively); however, compared to the muscle model group, the force generator group's movement times became shorter after the dynamics switch (group main effect: $p < .005$). Note that this does not necessarily indicate better performance because the virtual limb stops sooner on undershoots compared to overshoots that move further past the target. There were no overall practice effects or interactions for movement time, error, and performance ($p > .10$).

Discussion

If the nervous system has knowledge of muscle dynamics, it was hypothesized that subjects who practiced controlling a virtual limb with virtual muscle actuators would improve performance faster and show greater generalization than those who learned with force generator actuators. On the other hand, if subjects do not leverage their knowledge of muscle dynamics, the force generator group was expected to show faster improvement and better generalization because the force generator requires a mathematically simpler transformation from neural activation to force. The results provided partial support for the hypothesis: there were no differences in the learning rate between the groups; however, the muscle model group showed better generalization than the force generator group, but only in early skill acquisition. Each of these findings and the degree to which they are consistent with a neural representation of muscle dynamics is now discussed.

Task performance and generalization

Despite using markedly different actuators, there were no learning rate differences between the muscle model and force generator groups. This is noteworthy because the differences between actuator model dynamics were not minor. As demonstrated by the dynamics-switch trials, failure to plan for the correct actuator model caused (or would have caused without corrective actions) significant end-point errors. This raises the question: why did subjects who used the more complex muscle model learn just as fast as those who learned with the simpler force generator?

It was expected that if subjects were truly *tabula rasas*, i.e., they had no prior knowledge of muscle dynamics, subjects who practiced with the muscle model would have had *more* difficulty learning the task compared to subjects who used the simpler force generator. This follows Narain et al. (2013), who demonstrated that more complex models of dynamics require more time to learn than simpler models. A preexisting neural representation of muscle dynamics may have provided a jump start on the learning process, negating the learning rate penalty that would normally be expected with more complex dynamics. Note that here "complexity" is operationally defined in terms of the input–output behavior of the two actuator models: the muscle model force is dependent on several nonlinear functions but the force generator force depends on a single linear function. What the nervous system views as "complex" cannot be answered in the present study.

An alternative explanation for lack of learning rate differences is that the intrinsic stabilizing properties of muscle could have simplified control (Brown and Loeb 1999), mitigating the learning rate penalty associated with more complex dynamics. However, active stabilization of the virtual limb did not play a large role in the present study. There were no unexpected force perturbations to the virtual limb, and end-point stabilization was not necessary because the modeled frictional forces brought the limb to a stop. Also, since there was only one muscle subjects could not modulate the virtual limb's impedance through co-activation of antagonist muscles (Hogan 1984).

Turning now to the generalization of performance, the hypothesis was supported as the muscle model group had improved performance transfer compared to the force generator group, but only in early practice. Improved early practice generalization suggests that subjects' prior experience controlling muscles may have provided an advantage in interpolating/extrapolating their muscle activation strategies to new task configurations. However, the group generalization differences were washed-out as subjects became more practiced in the task. This could be because the early generalization trials were a more accurate reflection of the "initial conditions," i.e., what neural representation(s) subjects possessed before the experiment. Any advantage that this may have provided the muscle model group early in practice may have been diminished as the force generator group continued to practice the task.

Although the critical comparison was between the muscle model and force generator groups, the exceptional performance transfer exhibited by the muscle model group in early practice is notable. This is consistent with others who have studied relatively simple tasks and showed nearly complete generalization of performance (Gordon et al. 1994; Morton et al. 2001). However, for the near target, the muscle model group appeared to have *greater* performance compared to the standard trials. This is in part due to nonlinearities in the early standard trial practice data, i.e., disproportionally large errors were made on the very early trials, a typical feature of motor learning. Because the

performance measures for the generalization trials were relative to the standard trials, these larger initial errors inflate the average early practice error and exaggerate the degree of generalization. When the analysis was redone excluding the very early practice trials (first 5 trials), generalization for the near and far targets decreased, but the group differences remained. Another factor contributing to the high degree of generalization for the near target is that subjects had less distance to move, which would tend to decrease error and therefore increase the performance measure.

It was also observed that as both groups progressed in the practice session, performance on the far target steadily declined, but near-target performance remained relatively flat after the first practice block. This could be because as subjects become more skilled they make less overshoot errors and therefore pass through the far target less frequently compared to the near target. As practice progresses, subjects continue to move through states associated with the near target, but have fewer exposures to the far-target states. Therefore, subjects maintained comparatively better performance on the near-target generalization trials.

Task sensitivity to actuator dynamics

A prerequisite to testing the hypothesis was to verify that performance of the task was sensitive to the properties of the actuator models. That is, subjects should make significant errors if the actuator dynamics are unexpectedly changed after adaptation. When the muscle model actuator was switched to a force generator, subjects made large overshoot errors. With the muscle model, force is depressed upon initial activation because the CE shortens rapidly as it begins to produce force and stretches the series elastic element. Since the force generator did not have a force–velocity relation or series elastic element, force rose faster than anticipated after the dynamics switch. This caused the virtual limb to accelerate rapidly and quickly pass a point where it could not be stopped before passing the target (e.g., Fig. 8d), as there was no antagonistic actuator to actively brake the virtual limb or pull it back to the target once passed.

In the force generator to muscle model switch, instead of force rising in lockstep with activation, which occurred with the force generator model, the shortening of the suddenly present CE made the limb respond more sluggishly, producing less force initially and throughout limb movement due to force–length–velocity properties. This unexpected force depression will cause an undershoot, which can be corrected with additional control inputs, reducing the final end-point error. To address this in trials with undershoot corrections, virtual limb movement was simulated to see where the limb would have ended up without the correction. This showed that the subjects would have indeed made undershoot errors, supporting the conclusion that task performance was sensitive to the actuator dynamics.

The observed under/overshoot errors are consistent with a motor plan tuned to the dynamics of a particular actuator model, which became inappropriate when the dynamics were altered. In principle, this effect is similar to what is observed for catch trials in experiments that apply force fields (Gandolfo et al. 1996) or visuo-motor rotations (Caithness et al. 2004), which cause directionally specific movement errors that are gradually eliminated with motor adaptation. In those paradigms, when the manipulation is turned off, an aftereffect is observed that causes error to increase in a direction opposite to the pre-adapted state and is cited as evidence for model-based prediction (Shadmehr and Mussa-Ivaldi 1994). In the present study, the virtual dynamics could not be turned off, only switched from one form to another.

Limitations

There are several limitations that should be considered when interpreting the results of this study: (1) Although the muscle model had force–length, force–velocity, and force–extension relations, many other properties were not included, e.g., history-dependent force enhancement and depression (Edman et al. 1978, 1993). Also, architectural properties such as pennation angle, which influence fiber shortening velocities, were not modeled (Spector et al. 1980). (2) The virtual task aimed to mimic actions performed in everyday activities that do not involve high forces, e.g., comfortable-speed elbow flexion movements elicit biceps muscle activation below 10 % of maximum (Koo and Mak 2005). Experimental outcomes may be different for tasks that drive actuators near their force-generating limits. (3) Proprioceptive information about the state of the virtual muscle and limb was absent. This limitation is shared by recent studies using virtual limbs (e.g., de Rugy et al. 2012). Even though the proprioceptive information was missing, this was consistent among the experimental groups, and subjects in both groups were able to significantly improve their control of the virtual limb. This supports the ability of humans to acquire internal models of external dynamics with only visual feedback (Radhakrishnan et al. 2008). (4) Generalization was only tested over a limited range. Previous work has shown that generalization usually decreases as task conditions deviate further from the trained condition (Donchin et al. 2003). It is unclear whether the results will hold under more extreme generalization tests. (5) Subjects had to learn virtual limb dynamics in addition to actuator dynamics. However, any group differences in performance can be ascribed to actuator dynamics because the virtual limb dynamics (i.e.,

inertial properties and passive torques) were identical across experimental groups. Removing the limb dynamics, for instance, by having subjects learn to control an abstract representation of force amplitude (e.g., Gordon and Ferris 2004), would detract from in vivo conditions, in which muscles are attached to articulated limbs. (6) The virtual limb model was a grossly simplified model of a human limb; the results may change with a more complex model. Making the virtual limb model more complex, for example, by adding more muscles, muscle properties, or kinematic degrees-of-freedom, would increase physiological accuracy, but may do so at the cost of decreasing the interpretability of the data. Because of these reasons, and because this study represents an initial test of the hypothesis, a simple model was used.

Considerations

There are two considerations related to the experimental design that merit discussion. The first is whether simultaneous sensory feedback from the actual and virtual limbs influenced subjects' perception of the task, which could in turn affect the results. The virtual limb feedback shows a moving limb, but feedback from the actual limb signals a stationary limb (subjects' limbs were restrained). While this discrepancy would make it difficult to convince participants that the virtual limb movements reflected those of their actual limb, this was not the goal of the present study and was not a requirement for testing the hypothesis. The second consideration relates to how subjects used error information to improve their performance in the virtual limb task. Between the actual and virtual limbs, only the virtual limb display provided error information pertinent to the task goal, and therefore, only the virtual limb feedback should have been used to correct the actions of the virtual limb minimum intervention principle; Todorov and Jordan 2002a. While subjects also received feedback from their own limbs, the states (positions and velocities) of their limbs did not affect the task goal. Only the biceps-derived activation signal was causally linked to the movement of the virtual limb and task goal.

Conclusions

This study represents an initial investigation into whether the nervous system accounts for muscle dynamics in voluntary movement control. The results demonstrated that when learning to control a virtual limb, subjects who used muscle models, in which the actuation force was a function of nonlinear force–length–velocity relations and a series elastic stiffness, learned at the same rate as those whose muscle activity was directly translated into a force via a simple force generator. In addition, during early skill acquisition, subjects using the muscle model were better able to transfer what they learned to different task conditions, but this advantage was lost with practice. Together, these results are consistent with a preexisting neural representation of muscle dynamics. If subjects had no prior neural representation of muscle dynamics, the more challenging muscle model dynamics should have taken longer to learn and been more difficult to generalize, but familiarity with muscle function may have offset this disadvantage.

Acknowledgments Thanks to Annalisa Hamel-Smith and Conor Bray for their assistance with data collection, and Sheng-Che Yen and anonymous reviewers for critical and insightful comments.

References

Akaike H (1974) A new look at the statistical model identification. IEEE Trans Autom Control 19:716–723

An K, Ueba Y, Chao E, Cooney W, Linscheid R (1983) Tendon excursion and moment arm of index finger muscles. J Biomech 16:419–425

Armstrong B, de Wit CC (1996) Friction modeling and compensation. In: The control handbook, vol 77, pp 1369–1382

Asmussen E, Bonde-Petersen F (2008) Storage of elastic energy in skeletal muscles in man. Acta Physiol Scand 91:385–392

Atkeson CG (1989) Learning arm kinematics and dynamics. Ann Rev Neurosci 12:157–183

Bahler AS (1967) Series elastic component of mammalian skeletal muscle. Am J Physiol 213:1560–1564

Brainard DH (1997) The psychophysics toolbox. Spat Vis 10:433–436

Brown IE, Loeb GE (1999) A reductionist approach to creating and using neuromusculoskeletal models. In: Winters J, Crago P (eds) Biomechanics and neural control of movement. Springer-Verlag, New York, pp 148–163

Caithness G, Osu R, Bays P et al (2004) Failure to consolidate the consolidation theory of learning for sensorimotor adaptation tasks. J Neurosci 24:8662–8671

Cavagna GA (1977) Storage and utilization of elastic energy in skeletal muscle. Exerc Sport Sci Rev 5:89–130

Cheng EJ, Loeb GE (2008) On the use of musculoskeletal models to interpret motor control strategies from performance data. J Neural Eng 5:232

Conditt MA, Gandolfo F, Mussa-Ivaldi FA (1997) The motor system does not learn the dynamics of the arm by rote memorization of past experience. J Neurophysiol 78:554–560

de Rugy A, Loeb GE, Carroll TJ (2012) Muscle coordination is habitual rather than optimal. J Neurosci 32:7384–7391

Dingwell JB, Mah CD, Mussa-Ivaldi FA (2002) Manipulating objects with internal degrees of freedom: evidence for model-based control. J Neurophysiol 88:222–235

Donchin O, Francis JT, Shadmehr R (2003) Quantifying generalization from trial-by-trial behavior of adaptive systems that learn with basis functions: theory and experiments in human motor control. J Neurosci 23:9032–9045

Edman K, Elzinga G, Noble M (1978) Enhancement of mechanical performance by stretch during tetanic contractions of vertebrate skeletal muscle fibres. J Physiol 281:139–155

Edman K, Caputo C, Lou F (1993) Depression of tetanic force induced by loaded shortening of frog muscle fibres. J Physiol 466:535–552

Erdemir A, McLean S, Herzog W, van den Bogert AJ (2007) Model-based estimation of muscle forces exerted during movements. Clin Biomech 22:131–154

Feldman AG (1966) Functional tuning of the nervous system with control of movement or maintenance of a steady posture, II: controllable parameters of the muscles. Biophysics 11:565–578

Fellows S, Rack P (1987) Changes in the length of the human biceps brachii muscle during elbow movements. J Physiol 383:405–412

Flanagan JR, Wing AM (1997) The role of internal models in motion planning and control: evidence from grip force adjustments during movements of hand-held loads. J Neurosci 17:1519–1528

Gandolfo F, Mussa-Ivaldi F, Bizzi E (1996) Motor learning by field approximation. Proc Natl Acad Sci 93:3843–3846

Gerritsen KG, van den Bogert AJ, Hulliger M, Zernicke RF (1998) Intrinsic muscle properties facilitate locomotor control—a computer simulation study. Mot Control 2:206–220

Gordon KE, Ferris DP (2004) Proportional myoelectric control of a virtual object to investigate human efferent control. Exp Brain Res 159:478–486

Gordon A, Huxley AF, Julian F (1966) The variation in isometric tension with sarcomere length in vertebrate muscle fibres. J Physiol 184:170–192

Gordon AM, Forssberg H, Iwasaki N (1994) Formation and lateralization of internal representations underlying motor commands during precision grip. Neuropsychologia 32:555–568

Hall E, Flament D, Fraser C, Lemon R (1990) Non-invasive brain stimulation reveals reorganised cortical outputs in amputees. Neurosci Lett 116:379–386

Hasson CJ, Caldwell GE (2012) Effects of age on mechanical properties of dorsiflexor and plantarflexor muscles. Ann Biomed Eng 40:1088–1101

Hasson CJ, Shen T, Sternad D (2012) Energy margins in dynamic object manipulation. J Neurophysiol 108:1349–1365

Hatze H (1975) A new method for the simultaneous measurement of the moment of inertia, the damping coefficient and the location of the centre of mass of a body segmentin situ. Eur J Appl Physiol Occup Physiol 34:217–226

Hill A (1938) The heat of shortening and the dynamic constants of muscle. Proc R Soc B 126:136–195

Hof A (2003) Muscle mechanics and neuromuscular control. J Biomech 36:1031–1038

Hogan N (1984) Adaptive control of mechanical impedance by coactivation of antagonist muscles. IEEE Trans Autom Control 29:681–690

Hooper SL, Weaver AL (2000) Motor neuron activity is often insufficient to predict motor response. Curr Opin Neurobiol 10:676–682

Jordan MI, Rumelhart DE (1992) Forward models: supervised learning with a distal teacher. Cogn Sci 16:307–354

Kawato M (1990) Feedback-error-learning neural network for supervised motor learning. In: Eckmiller R (ed) Advanced neural computers. North-Holland, Amsterdam, pp 365–372

Kistemaker DA, Van Soest AJK, Wong JD, Kurtzer I, Gribble PL (2013) Control of position and movement is simplified by combined muscle spindle and Golgi tendon organ feedback. J Neurophysiol 109:1126–1139

Koo TK, Mak AF (2005) Feasibility of using EMG driven neuromusculoskeletal model for prediction of dynamic movement of the elbow. J Electromyogr Kinesiol 15:12–26

Kubow T, Full R (1999) The role of the mechanical system in control: a hypothesis of self-stabilization in hexapedal runners. Philos Trans R Soc B 354:849–861

Kuiken T, Dumanian G, Lipschutz R, Miller L, Stubblefield K (2004) The use of targeted muscle reinnervation for improved myoelectric prosthesis control in a bilateral shoulder disarticulation amputee. J Prosthet Orthot Int 28:245–253

Kurtzer IL, Pruszynski JA, Scott SH (2008) Long-latency reflexes of the human arm reflect an internal model of limb dynamics. Curr Biol 18:449–453

Manal K, Gonzalez RV, Lloyd DG, Buchanan TS (2002) A real-time EMG-driven virtual arm. Comp Biol Med 32:25–36

Miall R, Weir D, Wolpert D, Stein J (1993) Is the cerebellum a Smith predictor? J Mot Behav 25:203–216

Morton SM, Lang CE, Bastian AJ (2001) Inter- and intra-limb generalization of adaptation during catching. Exp Brain Res 141:438–445

Narain D, Mamassian P, Brenner E, Smeets J, van Beers R (2013) The acquisition of hidden models in sensorimotor learning. In: 23rd annual meeting on the neural control of movement, San Juan, Puerto Rico, 16-20 April 2013

Ostry DJ, Feldman AG (2003) A critical evaluation of the force control hypothesis in motor control. Exp Brain Res 153:275–288

Potvin J (1997) Effects of muscle kinematics on surface EMG amplitude and frequency during fatiguing dynamic contractions. J Appl Physiol 82:144–151

Press WH, Teukolsky SA, Vetterling WT, Flannery BP (2007) Numerical recipes: the art of scientific computing, 3rd edn. Cambridge University Press, Cambridge

Radhakrishnan SM, Baker SN, Jackson A (2008) Learning a novel myoelectric-controlled interface task. J Neurophysiol 100:2397–2408

Reis J, Schambra HM, Cohen LG et al (2009) Noninvasive cortical stimulation enhances motor skill acquisition over multiple days through an effect on consolidation. Proc Natl Acad Sci 106:1590–1595

Sainburg R, Ghez C, Kalakanis D (1999) Intersegmental dynamics are controlled by sequential anticipatory, error correction, and postural mechanisms. J Neurophysiol 81:1045–1056

Schwarz G (1978) Estimating the dimension of a model. Ann Stat 6:461–464

Shadmehr R, Mussa-Ivaldi FA (1994) Adaptive representation of dynamics during learning of a motor task. J Neurosci 14:3208–3224

Shmuelof L, Huang VS, Haith AM, Delnicki RJ, Mazzoni P, Krakauer JW (2012) Overcoming motor "forgetting" through reinforcement of learned actions. J Neurosci 32:14617–14621a

Smith MA, Ghazizadeh A, Shadmehr R (2006) Interacting adaptive processes with different timescales underlie short-term motor learning. PLoS Biol 4:e179

Spector SA, Gardiner PF, Zernicke RF, Roy RR, Edgerton V (1980) Muscle architecture and force–velocity characteristics of cat soleus and medial gastrocnemius: implications for motor control. J Neurophysiol 44:951–960

Svinin M, Goncharenko I, Luo Z-W, Hosoe S (2006) Reaching movements in dynamic environments: how do we move flexible objects? IEEE Trans Robot 22:724–739

Todorov E, Jordan MI (2002a) A minimal intervention principle for coordinated movement. In: Becker S, Thrun S, Obermayer K (eds) Advances in neural information processing systems, vol 15. MIT, Cambridge, MA, pp 27–34

Todorov E, Jordan MI (2002b) Optimal feedback control as a theory of motor coordination. Nat Neurosci 5:1226–1235

Winters JM, Stark L (1988) Estimated mechanical properties of synergistic muscles involved in movements of a variety of human joints. J Biomech 21:1027–1041

Wolpert DM, Ghahramani Z (2000) Computational principles of movement neuroscience. Nat Neurosci 3:1212–1217

Wolpert DM, Kawato M (1998) Multiple paired forward and inverse models for motor control. Neural Netw 11:1317–1329

Zajac FE (1989) Muscle and tendon: properties, models, scaling, and application to biomechanics and motor control. Crit Rev Biomed Eng 17:359–411